Vision, Modeling, and Visualization (2010)

# Application of Tensor Approximation on Multiscale Volume Feature Representations

S.K. Suter[1,2], and C.P.E. Zolikofer[2] and R. Pajarola[1]

[1]Department of Informatics, University of Zurich, Switzerland
[2]Anthropological Institute and Museum, University of Zurich, Switzerland

**Abstract**

*Advanced 3D microstructural analysis in natural sciences and engineering depends ever more on modern data acquisition and imaging technologies such as micro-computed or synchrotron tomography and interactive visualization. The acquired volume data sets are not only of high-resolution but in particular exhibit complex spatial structures at different levels of scale (e.g. variable spatial expression of multiscale periodic growth structures in tooth enamel). Such highly structured volume data sets represent a tough challenge to be analyzed and explored by means of interactive visualization due to the amount of raw volume data to be processed and filtered for the desired features. As an approach to address this bottleneck by multiscale feature preserving data reduction, we propose higher-order tensor approximations (TAs). We demonstrate the power of TA to represent, and highlight the structural features in volume data. We visually and quantitatively show that TA yields high data reduction and that TA preserves volume features at multiple scales.*

Categories and Subject Descriptors (according to ACM CCS): I.3.3 [Computer Graphics]: Picture/Image Generation—Viewing algorithms I.4.7 [Computer Graphics]: Feature Measurement—Feature representation

## 1. Introduction

Non-invasive analysis of organismic structures, tissue and materials with microtomographic techniques has seen a rapid development over the past few years. Micro-computed X-ray tomography ($\mu$CT) has now become a standard tool, e.g., in bio-medical research. As a relatively recent technology, Synchrotron Tomography (ST) has opened up new areas of research at the sub-micrometer level. The resulting structural volume data sets exhibit an increasing structural complexity in space at different scales. The features we target in bio-medical tissue analysis are multiscale periodic patterns (e.g., of growth structures in tooth enamel).

Phase contrast Synchrotron Tomography (pcST) has become of special interest to the analysis of growth structures in hard tissues of living and fossil species [TS08]. For example, patterns of daily enamel deposition in fossil hominid teeth are imaged with pcST and counted to estimate the age at death of a fossil specimen. However, current approaches are restricted to the analysis of serial 2D cross sections through data volumes, while the actual growth microstructures have complex three-dimensional shapes [JSM03, MJS03]. Hence there is a need for tools to visualize 3D microstructural features at various scales.

The grand challenge today is thus to make the *implicit* information contained in structural volume data *explicitly* available. Since these internal structures are in the micrometer domain, the data size of one volume block typically exceeds the limits for interactive visualization on modern graphic systems. Therefore, preprocessing of the data sets prior to rendering for visual exploration is needed. Meeting this challenge not only requires solutions for large scale volume rendering, but more specifically a method to reduce the data set size and a method to represent multiscale volume features, which we investigate in this paper.

**Contributions** In this work, we demonstrate an application of low-rank tensor approximations as a common mathematical framework to: (a) extract relevant features from a structural volume data set, (b) reduce the size of the data set, and (c) visualize the internal 3D features at different spatial scales.

## 2. Related Work

In the context of visualization and exploration of large volume data there is an ongoing need to reduce and optimize the amount of data to be processed and displayed. A fundamental concept of data reduction is to remove redundant and irrelevant information while preserving the most relevant features. Techniques of data reduction are thus directly related to concepts of noise reduction and feature extraction.

Improving on the *Fourier Transform* (FT), the *Wavelet Transform* (WT) decomposes any input signal into a localized frequency domain. Today, the WT is a standard method for compressed volume data representation (e.g. [IP98, Rod99, KS99, NS01, GWGS02, SW03]). However, the bases retrieved from a classical WT multiresolution analysis are unaware of the 3D structures within the data sets. Even tough the basis coefficients of WT are adaptively obtained, the (separable) WT results from convolutions along the three major spatial axes *xyz* with predefined 1D filters, i.e., the data reduction ratio as well as the bases are defined by these axes. We therefore call these bases *axis-aligned bases*. However, significant features in structural volume data are typically not aligned along axes *xyz*, such that techniques are required which rather produce *feature-aware bases*. In fact, the basis functions, wavelet and scaling filters, are fixed for a given type of WT.

*Tensor-based approximations* (TAs) have become a significant research topic in data reduction and visualization [VT04, WWS*05, TS06, WA08, WXC*08, YWT*09]. TAs reduce the stored size of a data set, and simultaneously transform it into a compact multilinear representation. In essence, the TA represents an extension of the concept of principal components analysis (PCA) to multi-modal input data. One mode refers to one axis of the data set, e.g., to one of the *xyz* spatial axis in a volumetric data set. While the PCA computes the data correlations in two modes (covariances) the TA does it for $N$ modes (covariances along each mode). With a three-way [KDL80, Kro3c, TBDLK87] or $N$-way [dLdMV00a, dLdMV00b] analysis, the input data set is decomposed into multilinear components, the so called Tucker model [Tuc66], which consists of a core tensor and basis matrices along each mode. These components capture the signal's most important information in one corner of the core tensor. As in PCA, matrix covariances in TA reveal statistically relevant features in the data set. We thus use the term *feature-aware bases*. In contrast to WT, the basis functions in TA are found adaptively based on the input data.

To illustrate the specific properties of the TA approach, let us recall that recursive application of WT yields a *multiresolution analysis* of the input data set. As such, the WT defines a multiresolution hierarchy of coefficients. Each coefficient is responsible to improve the approximation of the original data over a fixed area at a well defined location. Hence the WT is designed to minimize the mean scalar differences between approximated and original data at different spatial resolutions, where higher-level coefficients generally are more important (in energy terms). In contrast, the TA provides an approximation of the original data at multiple scales of data correlation, rather than at multiple spatial resolutions. This property is termed here *feature awareness*.

Up to now, TA has mainly been applied to image ensembles (e.g. [VT04, WA08, YWT*09]). Here we focus on the 3D feature-preserving properties of the TA approach and compare its performance with the WT approach. Features contained in image data can be represented with modes of increasing dimensionality. In PCA, features are expressed as a vector ($1^{st}$-order tensor); in image ensembles [WA08, YWT*09], features are expressed as a matrix ($2^{nd}$-order tensor). With the TA-approach, we express features in terms of a $3^{rd}$-order tensor.

## 3. Tensor Decomposed Volume Representation

We review a mathematical framework, which we use in order to define a compact feature-preserving data representation in the context of structural volume visualization. The TA framework can achieve this goal through the decomposition of the volume data into a reduced set of bases.

### 3.1. Tensor Decomposition and Approximation

A tensor is a mathematical concept for a higher-order generalization of an array: A vector is a $1^{st}$-order tensor, a matrix a $2^{nd}$-order tensor and a volume is a $3^{rd}$-order tensor. In tensor approximation approaches, the input volume data set $\mathscr{A}$ is represented as a $3^{rd}$-order tensor and is decomposed into a multilinear data representation (here the Tucker model). The data size is reduced on the Tucker model directly such that irrelevant (uncorrelated) data is removed and important features are preserved (truncation of bases). Based on this truncated Tucker model, the original data set is then reconstructed to its approximation $\tilde{\mathscr{A}}$ (see Figure 1).

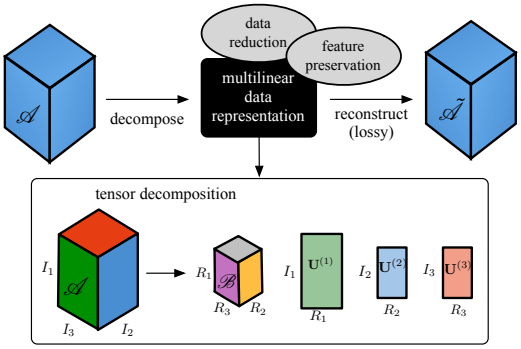


**Figure 1:** *Volume data approximation with $3^{rd}$-order TA.*

The multilinear data representation consists of one core tensor $\mathscr{B} \in \mathbb{R}^N$ and $N$ basis matrices $\mathbf{U}^{(1\ldots N)}$, where $N$

is the number of modes. A core tensor consists of coefficients, which show the level of interaction between different components; the basis matrices are usually orthogonal and can be thought of as principal components for each mode [KB09]. The maximum size of the decomposition is one core tensor with the same data size as the original input data $\mathscr{A} \in \mathbb{R}^{I_1 \times I_2 \cdots \times I_N}$, i.e., $\prod_{n=1}^{N} I_n$, and quadratic basis matrices for each mode, e.g. $I_n \cdot I_n$ for $\mathbf{U}^{(n)}$, where $I_n$ is the length of a mode. However, this would not result in any data reduction. But since the core tensor is arranged such that it has its highest energy in one corner (all-orthogonality property of core, [dLdMV00a]), we can apply a rank reduction on the complete multilinear data representation and work on lower-rank-$(R_1, R_2, \ldots R_N)$ tensor approximations ($R_n \leq I_n$). I.e., we always assume a lossy reconstruction.

### 3.2. Reduced Rank Tensor Decomposition

In the TA approach, a multi-modal data array or tensor $\mathscr{A}$, is approximated by a reduced-rank tensor decomposition, i.e., the ranks of the core and the basis matrices are truncated. A tensor rank reduction is performed in a similar way like a matrix rank reduction (see [dLdMV00a]). For a real $N^{th}$-order tensor $\mathscr{A} \in \mathbb{R}^{I_1 \times I_2 \cdots \times I_N}$ of size $\prod_{n=1}^{N} I_n$, a reduced-rank approximation can be defined as follows:

A rank-$(R_1, R_2, \ldots R_N)$ approximation of $\mathscr{A}$ is formulated as finding a lower-rank tensor $\widetilde{\mathscr{A}} \in \mathbb{R}^{I_1 \times I_2 \cdots \times I_N}$ with $rank_k(\widetilde{\mathscr{A}}) = R_k \leq rank_k(\mathscr{A})$, where $rank_k(\mathscr{A})$ is the order of the vector space of the $n$-mode vectors of $\mathscr{A}$. The $n$-mode product in tensor analysis is a special case of the inner product in multilinear algebra (see [dLdMV00a]), i.e., the $n$-mode vectors of a tensor correspond to the row-vectors or column-vectors of a matrix. In general, a reduced-rank approximation is sought such that the least-squares difference is minimized:

$$\widetilde{\mathscr{A}} = \arg\min(\widetilde{\mathscr{A}}) \parallel \mathscr{A} - \widetilde{\mathscr{A}} \parallel^2.$$

The approximated tensor can be represented as $\widetilde{\mathscr{A}} = \mathscr{B} \times_1 \mathbf{U}^{(1)} \times_2 \mathbf{U}^{(2)} \cdots \times_N \mathbf{U}^{(N)}$ from the $n$-mode product $\times_n$ of the basis matrices and the core tensor in a given reduced rank space. Given that $(R_1, \ldots R_N)$ are sufficiently smaller than the initial data dimensions $(I_1, \ldots I_N)$, the core tensor $\mathscr{B} \in \mathbb{R}^{R_1 \times R_2 \cdots \times R_N}$ and the basis matrices $\mathbf{U}^{(n)} \in \mathbb{R}^{I_n \times R_n}$ lead to a compact approximation $\widetilde{\mathscr{A}}$ of the original tensor $\mathscr{A}$.

In Figure 2 we illustrate this tensor decomposition for a $3^{rd}$-order tensor, or 3D volume data set. Note that the three basis matrices $\mathbf{U}^{(n=1\ldots3)}$ represent a set of $R_n$ column vectors each of length $I_n$, and the core tensor $\mathscr{B}$ is a $3^{rd}$-order tensor of size $R_1 \times R_2 \times R_3$, where $R_n \leq I_n$.

### 3.3. Reconstruction

As mentioned before, the goal is to find a reduced-rank tensor $\widetilde{\mathscr{A}}$ that approximates a given input data set $\mathscr{A}$ with as little error $\varepsilon = \parallel \mathscr{A} - \widetilde{\mathscr{A}} \parallel^2$ as possible. We can interpret $\widetilde{\mathscr{A}} = \mathscr{B} \times_1 \mathbf{U}^{(1)} \times_2 \mathbf{U}^{(2)} \cdots \times_N \mathbf{U}^{(N)}$ as a weighted sum over outer vector products

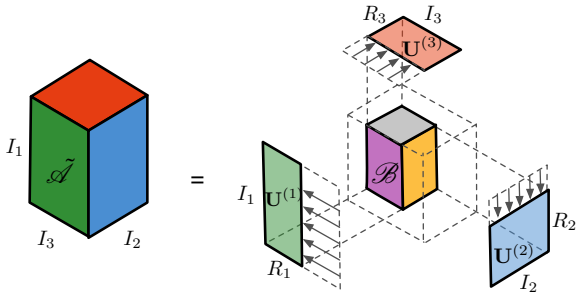


**Figure 2:** *Visualization of* $\widetilde{\mathscr{A}} = \mathscr{B} \times_1 \mathbf{U}^{(1)} \times_2 \mathbf{U}^{(2)} \times_3 \mathbf{U}^{(3)}$.

$$\widetilde{\mathscr{A}} = \sum_{r_k} \mathscr{B}[r_1, \ldots, r_N] \cdot \mathbf{U}^{(1)}_{(r_1)} \otimes \mathbf{U}^{(2)}_{(r_2)} \cdots \otimes \mathbf{U}^{(N)}_{(r_N)}, \quad (1)$$

with $\mathbf{U}_{(r)}$ indicating the $r$-th column vector of basis matrix $\mathbf{U}$ and the indices $r_k$ going from 1 to $R_N$ respectively. Intuitively, for every index combination $r_1, \ldots, r_N$ a $N^{th}$-order volume of original size is reconstructed by the outer-products, which is weighted for summation by the corresponding entry in the core tensor.

**Time and Space Cost** The basic formulation to reconstruct a 3D volume $\widetilde{\mathscr{A}}$ from its decomposition $\mathscr{B}$ and $\mathbf{U}^{(1..3)}$ is given in Equation 1, with $N = 3$. Given an original volume of size $I_1 \cdot I_2 \cdot I_3$ this equals to a weighted summation of $R_1 \cdot R_2 \cdot R_3$ such volumes. Instead of performing a naive reconstruction using $O(R_1 \cdot R_2 \cdot R_3 \cdot I_1 \cdot I_2 \cdot I_3)$ time, however, in practice an improved reconstruction is implemented, which computes the outer-products incrementally by rearranging the summation as follows,

$$\widetilde{\mathscr{A}} = \sum_r \mathbf{U}^{(1)}_{(r)} \otimes \sum_s \mathbf{U}^{(2)}_{(s)} \otimes \sum_t \mathscr{B}[r,s,t] \cdot \mathbf{U}^{(3)}_{(t)}, \quad (2)$$

resulting in a significantly reduced time cost of only $O(R_1 \cdot I_1 \cdot I_2 \cdot I_3)$. The order of the modes can be permuted such that $R_1$ has in fact the smallest rank, for overall best performance. The reduced-rank representation, consisting of the core tensor $\mathscr{B}$ and basis matrices $\mathbf{U}^{(1..3)}$, consumes $O(R_1 \cdot R_2 \cdot R_3 + R_1 \cdot I_1 + R_2 \cdot I_2 + R_3 \cdot I_3)$ space, in contrast to the $O(I_1 \cdot I_2 \cdot I_3)$ values of the original volume.

### 3.4. Multiscale and Progressive Reconstruction

With different rank-$(R_1, R_2, \ldots R_N)$ approximations of the original data volume $\mathscr{A}$, we achieve a progressive reconstruction. More precisely, we start with a tensor decomposition at a certain rank. By eliminating the least significant columns of the basis matrices and the corresponding data entries in the core tensor (= matrices, slices), reconstructions at a coarser respectively finer resolutions can be generated. The

tensor decomposition according to Equation 1 exhibits in its rank-space a natural order, where the ranks with a higher impact on the data set are generally ordered first. I.e., an initial high-quality tensor approximation with large rank dimensions $(R_1,\dots R_N)$ allows variable rank reconstruction using any index subranges $r_k \in 1\dots \leq R_k$, and hence it holds that:

$$\begin{aligned}\widetilde{\mathscr{A}_{R_k}} &= \sum_{r_k=1}^{R_k} \mathscr{B}[r_1,\dots,r_N]\cdot \mathbf{U}^{(1)}_{(r_1)} \otimes \mathbf{U}^{(2)}_{(r_2)} \cdots \otimes \mathbf{U}^{(N)}_{(r_N)} \\ &= \widetilde{\mathscr{A}_{R_k-1}} + \sum_{r_k=R_k-1}^{R_k} \mathscr{B}[r_1,\dots,r_N]\cdot \mathbf{U}^{(1)}_{(r_1)} \cdots \otimes \mathbf{U}^{(N)}_{(r_N)}\end{aligned}$$

With the concept of the rank reduction in the tensor decomposition, we have implicitly given a model for progressive reconstruction with one single tensor decomposition.

## 4. Implementation

For the application of TA to structural 3D volume data, there are three phases: (1) definition of the initial ranks $(R_1,R_2,R_3)$, (2) decomposition of the volume $\mathscr{A}$ into a core tensor $\mathscr{B}$ and three basis matrices $\mathbf{U}^{(1)},\mathbf{U}^{(2)}$, and $\mathbf{U}^{(3)}$, and (3) reconstruction of the volume $\widetilde{\mathscr{A}}$ from the reduced-rank tensor decomposition.

The progressive TA does not need to define a fixed set of reduced rank levels but can generate any lower rank reconstruction from a given initial rank-reduced starting point. We have chosen the ranks according to the scheme used in [WXC*08]: For the first approximation level, the ranks $(R_1,R_2,R_3)$ were chosen at half of the original dimensions $I_1\times I_2\times I_3$, i.e., the tensor decomposition is computed for the ranks $R_n=\frac{I_n}{2}$. This level achieves virtually accurate reconstruction, see also Section 5.3. For each subsequent step of rank reduction, the $R_n$ were further divided by 2 in a progressive way as described in Section 3.4. However, sometimes further refinements of the ranks can be performed since the choice of ranks is often done by comparing the approximations visually.

The tensor decomposition is usually implemented as an alternating least squares (ALS) algorithm on a higher-order singular value decomposition (HOSVD) [dLdMV00a] or a higher-order orthogonal iteration (HOOI) [dLdMV00b]. For the decomposition stage (2) in this work, the tensor decomposition is generated by the HOOI algorithm. The initial guess for the ALS was computed on eigenvalues.

For the reconstruction stage (3), outer-products of vectors and matrices according to Equations1 and 2 are used. Multiscale reconstructions at different rank-$(R_1,R_2,R_3)$ settings are computed incrementally as outlined in Section 3.4.

Readers interested in more details on the reduced-rank tensor approximations we refer to [dLdMV00a, dLdMV00b, Kro08, DLCM08, KB09].

## 5. Structural Volume Visualization

As outlined in the introduction, we searched for an approach to capture and identify the essential features of complex volumetric structures such as periodic growth patterns in tooth enamel in $\mu$CT or pcST imaging. In the following we define our multiscale features, compare the feature expressiveness of WT and TA, and demonstrate the effective feature-preserving reconstruction from TA.

### 5.1. Volume Features

Our structural volume *features* are defined by certain intensity regions, i.e., voxel elements $(i,j,k)$ for which their value $\mathscr{A}[i,j,k]$ is in a given interval, in the volume data set. The features we look at can manifest different characteristics at different scales. We interpret the feature scale-space in a traditional way such that at coarser scales only the larger and more prominent structural components should be maintained as features, and more detailed features are identified on finer scales. The *scale* in this context is given by the rank-$(R_1,R_2,R_3)$ reduction or number of coefficients used in the approximation $\widetilde{\mathscr{A}}$.

Feature expressiveness was evaluated visually as well as numerically. Visually, the coarsening and structural simplification of features can be verified by comparing the display of the original data set $\mathscr{A}$ to its approximation $\widetilde{\mathscr{A}}$. Numerically, we compared different approximations $\widetilde{\mathscr{A}_i}$ by their RMSE with respect to $\mathscr{A}$. Note however, that we are interested in the feature difference at a certain scale and thus the RMSE $E=\sqrt{m^{-1}\sum_{i,j,k}(\mathscr{A}[i,j,k]-\widetilde{\mathscr{A}}[i,j,k])^2}$ is computed one-sided, evaluated only for the $m$ voxels where $\widetilde{\mathscr{A}}[i,j,k]$ is within a given intensity range of interest.

### 5.2. Feature Expressiveness

To demonstrate the ability of TA to capture oriented patterns, we have applied the TA and the WT methods to various structural volume data sets containing multiscale features, and compared the performance of the two methods at corresponding approximation levels. For each approximation, the same number of non-zero coefficients (*NNC*) has been chosen for both the WT and TA method. For TA, *NNC* is given by the rank reduction as $R_1\cdot R_2\cdot R_3+R_1\cdot I_1+R_2\cdot I_2+R_3\cdot I_3$, representing the number of coefficients in the tensor decomposition. Correspondingly, we selected the *NNC* most significant wavelet coefficients (WCs). Unless specified otherwise, we used the multilevel biorthogonal 9/7 wavelet transform, which is also used in JPEG-2000 and in [WXC*08].

#### 5.2.1. Periodic Microstructures

The dental enamel data set is interesting since it represents periodic growth structures that occur at different levels of scale, and exhibit different spatial orientations. Human tooth enamel has a microstructure that is roughly comparable to

a bunch of densely packed fibers (so-called prisms, see Figure 4). During dental enamel formation, each dental enamel prism elongates in centrifugal direction through the daily apposition of a small segment of enamel. Daily growth increments are visible as surfaces perpendicular to the longitudinal direction of the prisms. In addition, approximately weekly growth halts are visible as so-called Retzius lines. As shown in Figure 3, the spatial scale and orientation of these structures is highly characteristic for each feature. This volume data set thus represents an ideal test case to assess the performance of TA as a feature-aware method compared to WT as an axis-aligend method.

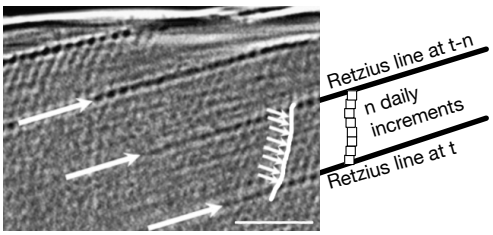


**Figure 3:** *Cross-sectional image of tooth enamel (pcST scan; scale = 50 microns) [TS08]. Small arrows: cross striations; large arrows: Retzius lines. The direction of the growth prisms is orthogonal to the cross striations.*

The images in Figure 4 demonstrate the reconstruction differences between WT and TA for simulated dental growth patterns (generated after [JSM03, MJS03]). The first and second row show approximated volumes with $NNC = 2'195'500$ and $958'500$ coefficients, corresponding to the size of rank-(128,128,128) and rank-(96,96,96) TAs respectively (Figure 4(e)). As can be seen in Figure 4(b), the simple Haar wavelet was able to reconstruct the original structures with $2'195'500$ NNCs, however, with $958'500$ NNCs, the structures dissolve. Besides that, Figure 4(b) shows that axis-aligned structures like e.g. the middle part of the simulated growth structure can be reconstructed with fewer coefficients than the curved structures. Other more complex wavelets like the biorthogonal 9/7 or Daubechies3 wavelets, have difficulties to reconstruct the original structures with $2'195'500$ NNCs (see Figures 4(c) and 4(d)). The third row, Figure 4(f-j), shows lower-rank TAs. As can be seen in Figure 4(g), TA still achieves to reconstruct the simulated growth structures faithfully with a low-rank-(32,32,32) TA, which is equal to $\frac{1}{300}$ of the original data elements (using $57'344$ NNCs).

Results of TA application to real microstructural data of tooth enamel are shown in Figures 5 and 6. Figure 5 demonstrates that a compact TA (rank-(8,8,8) with 2'048 coefficients) permits to highlight features (growth prisms) that are difficult to identify and visualize in the original data set, or on finer approximation scales. At corresponding number of coefficients, the Haar or biorthogonal 9/7 WT approaches show difficulties in reconstructing the characteristic features.

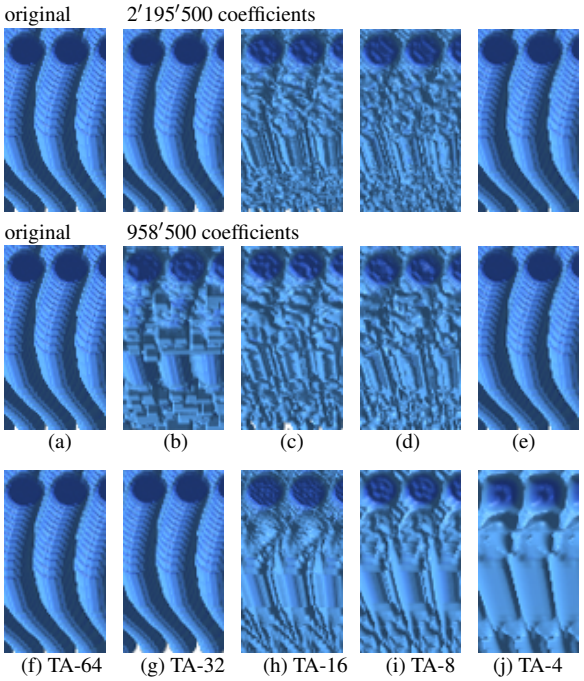


**Figure 4:** *(a) Original. Reconstruction using (b) Haar WT, (c) Biorthogonal 9/7 WT, (d) Daubechies3 WT and (e) TA. (f-j) Low-rank-$(R_k, R_k, R_k)$ TAs, for $R_k = 64, 32, 16, 8$ and 4.*

Figure 6 visualizes 3D dental enamel growth patterns as discussed previously and illustrated in Figure 3. The periodic halts along growth prisms cause the formation of surface layers, which can be identified and visualized using TA at different scales using progressive rank-reduction. In particular, the weekly growth markers (Retzius lines) can better be analyzed using 3D visualization and variation of reconstruction scale. The WT based approach fails to extract the growth-halt layers and continuously transforms into a blobby reconstruction at progressively reduced approximation level.

### 5.2.2. Multiscale Features

The bonsai tree volume represents a complex object structure with conspicuous features at multiple scales: trunk, branches, and leaves. An effective multiscale approach should be able to characterize these object parts as a function of the data reduction level. Ideally, the specific features should turn on and off on their adequate respective levels. Figure 7 shows the comparison of TA and a seven-level WT at corresponding numbers of coefficients. A high-quality approximation at half of the original ranks for TA and corresponding number of WCs, shows similar reconstructions in Figures 7(a) and 7(b). At lower rank reconstructions, however, the TA captures features of increasingly larger scale (Figures 7(d) and 7(f)), removing smaller variations in the data, while the WT rather approximates features at all scales

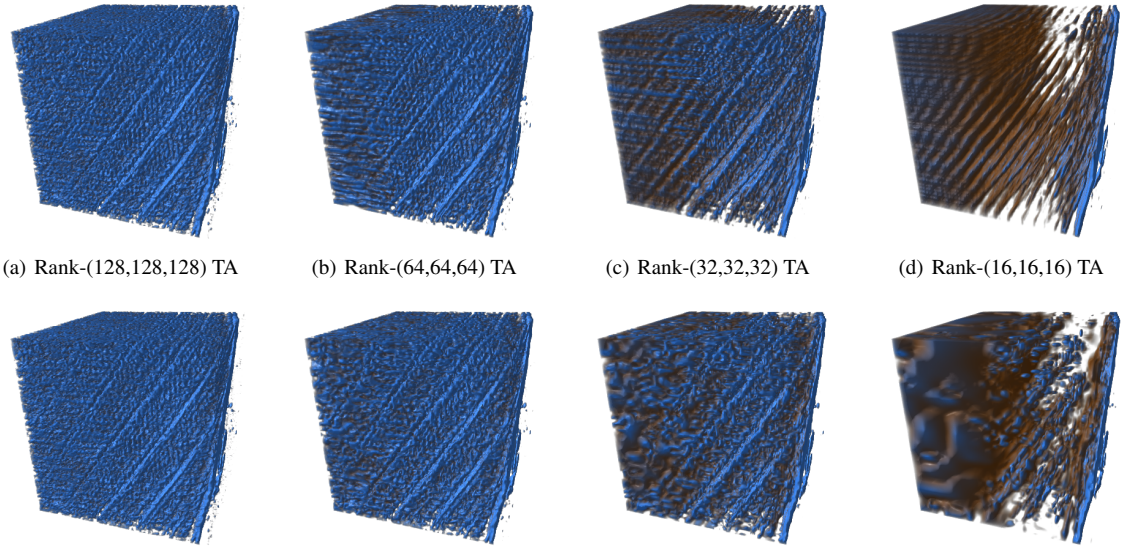

(a) Rank-(128,128,128) TA (b) Rank-(64,64,64) TA (c) Rank-(32,32,32) TA (d) Rank-(16,16,16) TA

(e) 2'195'456 WCs (f) 311'296 WCs (g) 57'344WCs (h) 16'384 WCs

**Figure 6:** *Periodic microstructures in tooth enamel ($256^3$, 16bit voxel depth, 0.75 microns per voxel). (a-d) Feature visualization using different rank-$(R_1,R_2,R_3)$ TAs. Showing on the front side, horizontal growth prisms oriented left-to-right and diagonal Retzius lines oriented bottom-left to top-right. (e-n) Reconstructions from corresponding numbers of biorthogonal 9/7 WCs.*

but at lower spatial resolution (Figures 7(c) and 7(e)). For pure visual approximation of objects, e.g. viewed from far, WT may be the optimal choice, but for structural analysis of features at different scales the TA may offer the better scale selectivity.

### 5.3. Rate-Distortion

Above we have presented a qualitative evaluation of the feature-preserving reconstruction performance of TA in comparison to state-of-the-art WT based approaches. In addition to the visual assessment of feature-expressiveness, a quantitative numerical approximation analysis is required to fully establish the capability and potential of the proposed TA based feature extraction and visualization framework. Our numerical evaluation analyzes the performance of TA versus WT in terms of its rate-distortion (Figure 8). As explained in Section 5.1, we measure the one-sided RMSE $E$ over all voxels in the intensity ranges indicating the selected features, and put $E$ in relation to the number of (non-zero) coefficients *NNC* used for different approximation levels.

As can be seen in Figure 8, for the Bonsai tree and the $256^3$ mictrostructure volume, the rate-distortion curves of TA and WT are close, with a slight advantage for the WT. On the other hand, for the $64^3$ microstructure volumes, the TA maintains a better rate-distortion in particular at lower reconstruction scales. Hence TA is as good in least-squares data approximation as WT.

## 6. Discussion and Conclusion

In [WWS*05, WXC*08], it has been shown that TA could generate higher quality images at larger data reduction ratios than WT or PCA. In our work, we went one step further and we have shown that the mathematical framework of TA permits to highlight features, which were difficult to see in the original data set (Figures 6(b) and 6(c)). This is in particular applicable for features at multiple scales, which can be brought out with TA at corresponding approximation levels (Figure 6). Notably at low-ranks, i.e., at high data reduction ratios, TA showed higher quality reconstructions of internal structures compared to WT.

While WT showed reconstructions with a closer visual resemblance to the overall original appearance, TA identifies specific structural features at different scales (e.g., Figures 6(b) or 6(d)). Wavelets focus on optimal data reduction over the complete volume. That is, WT is beneficial when the overall statistical distribution of the data set is intended to be reconstructed with a coarser resolution (Figure 7(e)). In contrast, we follow an approach that extracts specific features based on statistical properties like the major direction or a periodicity. TA, similar to PCA, which extracts the major direction of a data set, is more powerful regarding this latter aspect since it finds appropriate bases for reconstruction rather than assuming fixed basis functions as the WT. An approach like TA extracts components with more importance and neglects irrelevant areas within the data set. Hence TA is in advantage when we want to analyze features, e.g.,

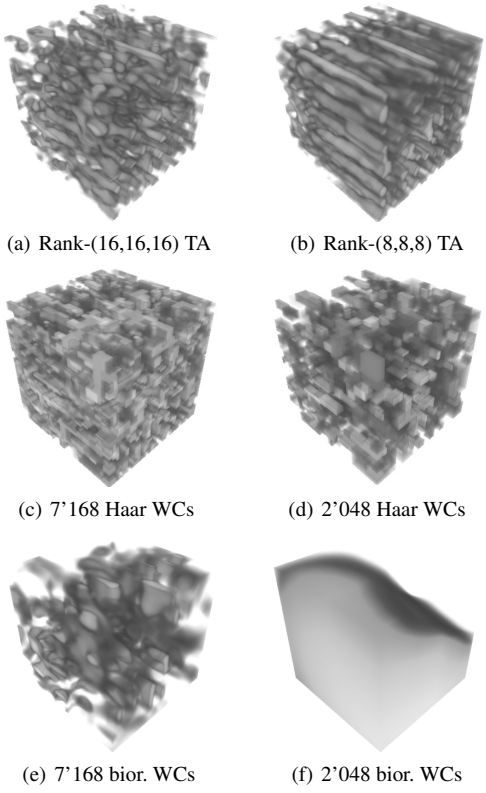

(a) Rank-(16,16,16) TA (b) Rank-(8,8,8) TA

(c) 7'168 Haar WCs (d) 2'048 Haar WCs

(e) 7'168 bior. WCs (f) 2'048 bior. WCs

**Figure 5:** *Structural volume data set of tooth enamel acquired with pcST ($64^3$ voxels, 16bit voxel depth, 0.75 microns resolution per voxel). Reconstructions from three different approximation levels: (a,b) TAs; (c,d) Haar WT, and (e,f) biorthogonal 9/7 WT.*

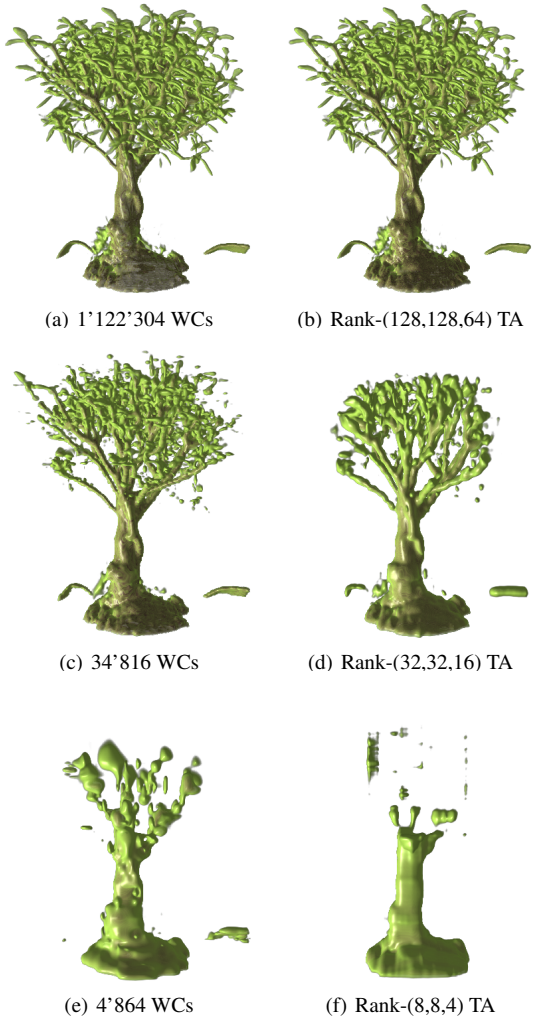

(a) 1'122'304 WCs (b) Rank-(128,128,64) TA

(c) 34'816 WCs (d) Rank-(32,32,16) TA

(e) 4'864 WCs (f) Rank-(8,8,4) TA

**Figure 7:** *The $256^2 \times 128$ bonsai tree approximated at different numbers of coefficients with WT (a,c,e) and TA (b,d,f).*

count the number of major branches of the tree (Figure 7(d)) or the Retzius lines in Figure 6(d).

Compared to wavelets, where different wavelets need to be evaluated in order to find out which wavelet fits best a data set, with the TA approach, we do not have to take such a decision, there is one mathematical tool, a rank-$(R_1, R_2, R_3)$ TA. However, higher computational cost need to be considered for TA (HOSVD/HOII), especially for large data sets, for which we need to consider bricking or similar data decomposition steps during volume processing and rendering.

We have also shown that classical measures of data reduction quality, such as rate-distortion, do not sufficiently capture the feature-expressiveness of a numerical approximation method. New procedures need to be developed, which permit the quantitative analysis of feature selectivity in lossy data reconstruction methods.

In summary, TA is powerful when we are not interested in the complete appearance of a data set, but rather want to highlight or count features at a certain scale. Since new data acquisition techniques lead to volume data sets of ever-increasing size, which tend to be one step ahead of the available graphics resources for interactive visualization, there is thus an ongoing need to develop new data reduction and feature extraction methods to tackle the resulting performance bottlenecks. This paper demonstrates that TA is a powerful approach to (a) represent microstructural volume data sets at high data reduction ratios, and (b) simultaneously highlight relevant features at different spatial scales.

**Acknowledgments**

The authors wish to thank volvis.org for the bonsai tree volume model and [TS08] for the image in Figure 3. Some of the images used in this paper have been generated us-

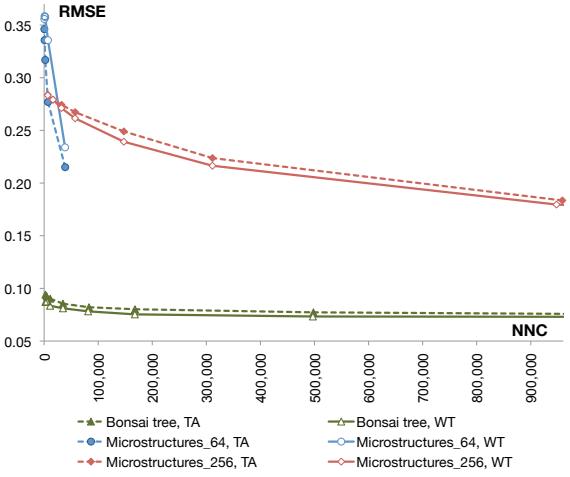


**Figure 8:** *Rate-distortion curves for TA and multilevel WT reconstructions for data sets from Figures 7, 5, and 6.*

ing the Voreen volume rendering engine (www.voreen.org) [MSRMH09]. Further, we want to mention the MatLab Tensor Toolbox [BK06], which served as a basis for our own implementation. This work was supported in part by the Forschungskredit of the University of Zurich, Switzerland.

## References

[BK06] BADER B. W., KOLDA T. G.: Algorithm 862: Matlab tensor classes for fast algorithm prototyping. *ACM Transactions on Mathematical Software 32*, 4 (2006), 635–653. 8

[DLCM08] DE LATHAUWER L., COMON P., MASTRONARDI N.: Special issue on tensor decompositions and applications. *SIAM Journal of Matrix Analysis and Applications 30*, 3 (2008), VII–VII. 4

[dLdMV00a] DE LATHAUWER L., DE MOOR B., VANDEWALLE J.: A multilinear singular value decomposition. *SIAM Journal of Matrix Analysis and Applications 21*, 4 (2000), 1253–1278. 2, 3, 4

[dLdMV00b] DE LATHAUWER L., DE MOOR B., VANDEWALLE J.: On the best rank-1 and rank-$(R_1, R_2, ..., R_N)$ approximation of higher-order tensors. *SIAM Journal of Matrix Analysis and Applications 21*, 4 (2000), 1324–1342. 2, 4

[GWGS02] GUTHE S., WAND M., GONSER J., STRASSER W.: Interactive rendering of large volume data sets. In *Proceedings IEEE Visualization* (2002), Computer Society Press, pp. 53–60. 2

[IP98] IHM I., PARK S.: Wavelet-based 3D compression scheme for very large volume data. In *Graphics Interface* (June 1998), pp. 107–116. 2

[JSM03] JIANG Y., SPEARS I. R., MACHO G. A.: An investigation into fractured surfaces of enamel of modern human teeth: a combined sem and computer visualisation study. *Archives of Oral Biology 48*, 6 (June 2003), 449–457. 1, 5

[KB09] KOLDA T. G., BADER B. W.: Tensor decompositions and applications. *SIAM Review 51*, 3 (2009), 455–500. 3, 4

[KDL80] KROONENBERG P., DE LEEUW J.: Principal component analysis of three-mode data by means of alternating least squares algorithms. *Psychometrika 45* (1980), 69–97. 2

[Kro08] KROONENBERG P. M.: *Applied Multiway Data Analysis*. Wiley's Series in Probability and Statistics, January 2008. 4

[Kro3c] KROONENBERG P. M.: *Three-mode principal component analysis: Theory and applications*. Leiden: DSWO Press, 1983c. 2

[KS99] KIM T.-Y., SHIN Y.-G.: An efficient wavelet-based compression method for volume rendering. In *Proceedings Pacific Graphics 99* (1999), pp. 147–156. 2

[MJS03] MACHO G. A., JIANG Y., SPEARS I. R.: Enamel microstructure – a truly three-dimensional structure. *Journal of Human Evolution 45*, 1 (July 2003), 81–90. 1, 5

[MSRMH09] MEYER-SPRADOW J., ROPINSKI T., MENSMANN J., HINRICHS K.: Voreen: A rapid-prototyping environment for ray-casting-based volume visualizations. *IEEE Computer Graphics and Applications 29*, 6 (2009), 6–13. 8

[NS01] NGUYEN K. G., SAUPE D.: Rapid high quality compression of volume data for visualization. In *Proceedings Eurographics* (2001), pp. 49–56. also in Computer Graphics Forum 20(3). 2

[Rod99] RODLER F.: Wavelet based 3D compression with fast random access for very large volume data. In *Proceedings Pacific Graphics* (1999), pp. 108–117. 2

[SW03] SCHNEIDER J., WESTERMANN R.: Compression domain volume rendering. In *Proceedings IEEE Visualization* (2003), pp. 293–300. 2

[TBDLK87] TEN BERGE J. M. F., DE LEEUW J., KROONENBERG P. M.: Some additional results on principal components analysis of three-mode data by means of alternating least squares algorithms. *Psychometrika 52* (1987), 183–191. 2

[TS06] TSAI Y.-T., SHIH Z.-C.: All-frequency precomputed radiance transfer using spherical radial basis functions and clustered tensor approximation. *ACM Transactions on Graphics 25*, 3 (2006), 967–976. 2

[TS08] TAFFOREAU P., SMITH T. M.: Nondestructive imaging of hominoid dental microstructure using phase contrast x-ray synchrotron microtomography. *Journal of Human Evolution 54*, 2 (February 2008), 272–8. 1, 5, 7

[Tuc66] TUCKER L. R.: Some mathematical notes on three-mode factor analysis. *Psychometrika 31*, 3 (September 1966), 279–311. 2

[VT04] VASILESCU M. A. O., TERZOPOULOS D.: Tensortextures: multilinear image-based rendering. *ACM Transactions on Graphics 23*, 3 (2004), 336–342. 2

[WA08] WANG H., AHUJA N.: A tensor approximation approach to dimensionality reduction. *International Journal of Computer Vision 76*, 3 (2008), 217–229. 2

[WWS*05] WANG H., WU Q., SHI L., YU Y., AHUJA N.: Out-of-core tensor approximation of multi-dimensional matrices of visual data. *ACM Transactions on Graphics 24*, 3 (August 2005), 527–535. 2, 6

[WXC*08] WU Q., XIA T., CHEN C., LIN H.-Y. S., WANG H., YU Y.: Hierarchical tensor approximation of multidimensional visual data. *IEEE Transactions on Visualization and Computer Graphics 14*, 1 (January/February 2008), 186–199. 2, 4, 6

[YWT*09] YAN S., WANG H., TU J., TANG X., HUANG T. S.: Mode-kn factor analysis for image ensembles. *IEEE Transactions on Image Processing 18*, 3 (March 2009), 670–676. 2